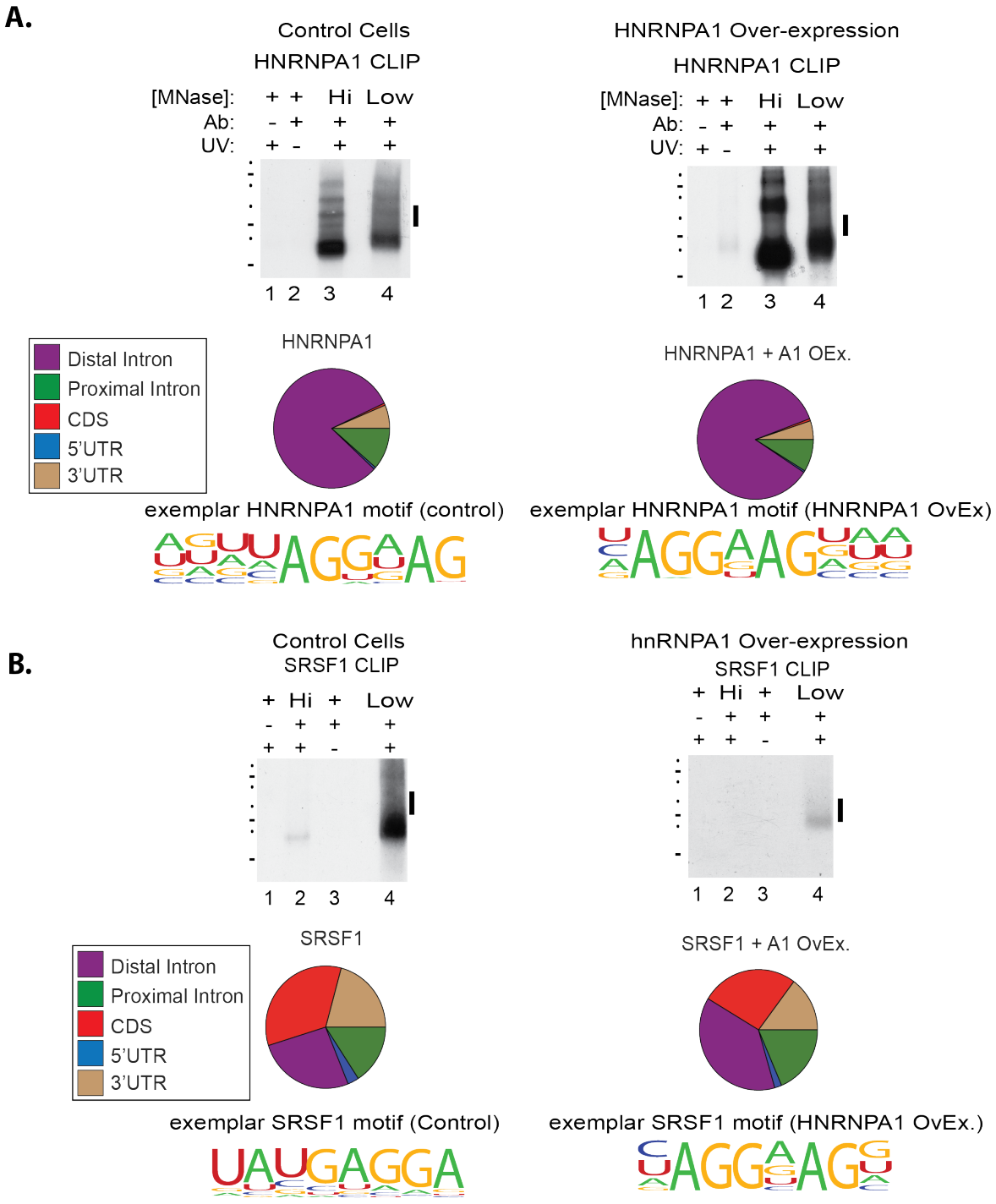

Supplemental Fig. 1. iCLIP analysis of HNRNPA1 and SRSF1 from control HEK 293 cells and HNRNPA1 over-expression cells. (A) Top left panel, autoradiograph from HNRNPA1 IP from control cells. Top left panel, autoradiograph from HNRNPA1 IP from HNRNPA1 over-expression cells. Middle left panel, annotation of HNRNPA1 peaks identified by CLIPper and consensus motifs identified by HOMER from control cells. Middle right panel, annotation of HNRNPA1 peaks identified by CLIPper and consensus motifs identified by HOMER from HNRNPA1 over-expression cells. **(B)** Top left panel, autoradiograph from SRSF1 IP from control cells. Top left panel, autoradiograph from SRSF1 IP from HNRNPA1 over-expression cells. Middle left panel, annotation of SRSF1 peaks identified by CLIPper and consensus motifs identified by HOMER from control cells. Middle right panel, annotation of SRSF1 peaks identified by CLIPper and consensus motifs identified by HOMER from HNRNPA1 over-expression cells.

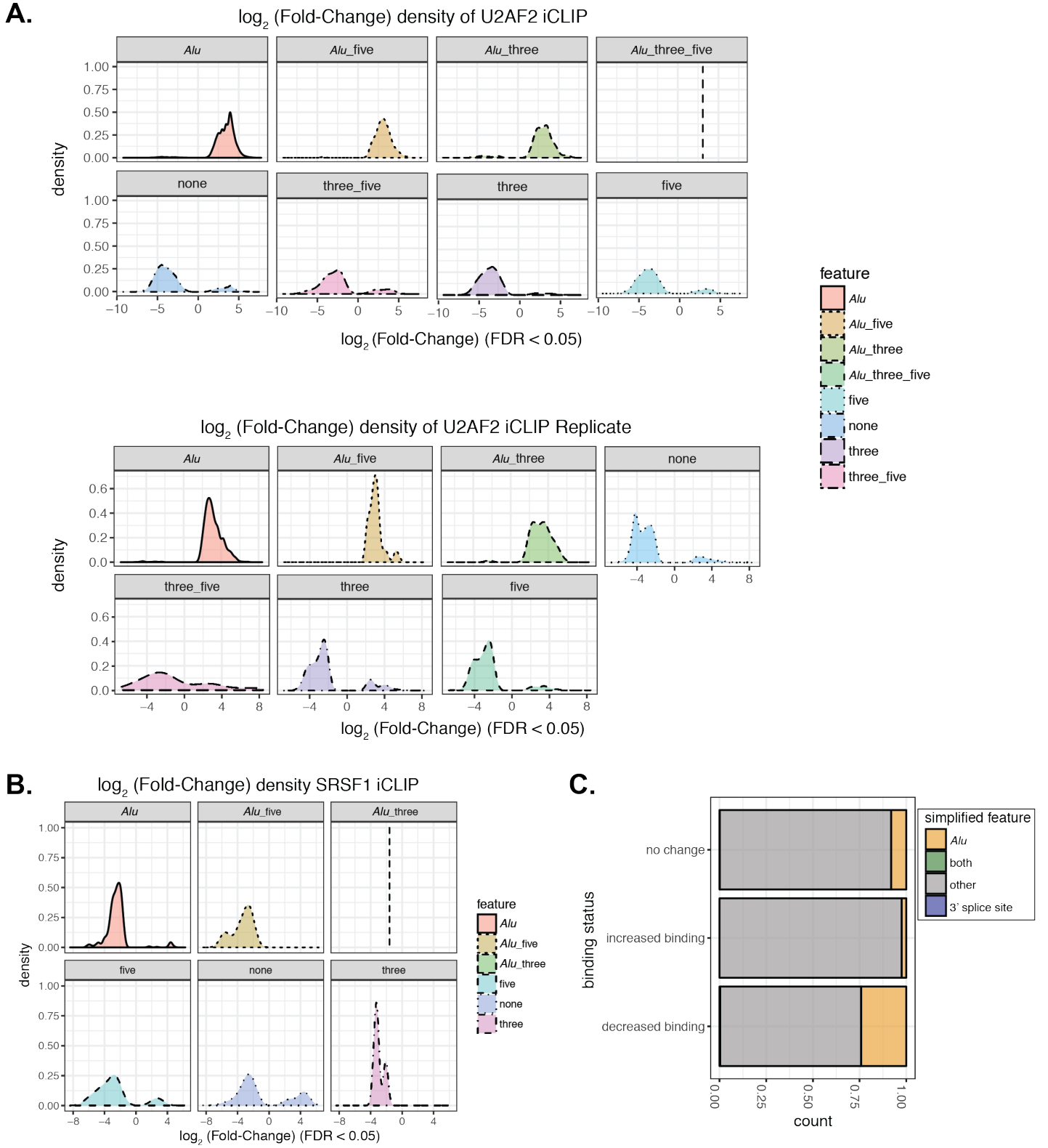

Supplemental Fig. 2. Distribution of changes to U2AF2 AND SRSF1 crosslinking peaks within specific genomic features. (A) Comparison of the density (y-axis) of crosslinking peaks with a given $\log_2$ (fold-change) between HNRNPA1 over-expression vs. control (x-axis) across multiple genomic features from two U2AF2 iCLIP experiments. **(B)** Comparison of the density (y-axis) of crosslinking peaks with a given $\log_2$ (fold-change) between HNRNPA1 over-expression vs. control (x-axis) across multiple genomic features from SRSF1 iCLIP experiment. **(C)** Stacked Bar graph showing the proportion of experiment of SRSF1 iCLIP crosslinking peaks showing No Change (top), Increased crosslinking peaks (Increased Binding) or decreased crosslinking peaks (Decreased Binding) associated with found within *Alu* elements, 3' splice site regions, both *Alu* and 3' splice site regions (both), or other regions outside of these (other). Peaks included in this plot have a $\log_2$ fold-change greater than -/+ 2 and a $-\log_{10}$ (adjusted p-value) less than 0.05.

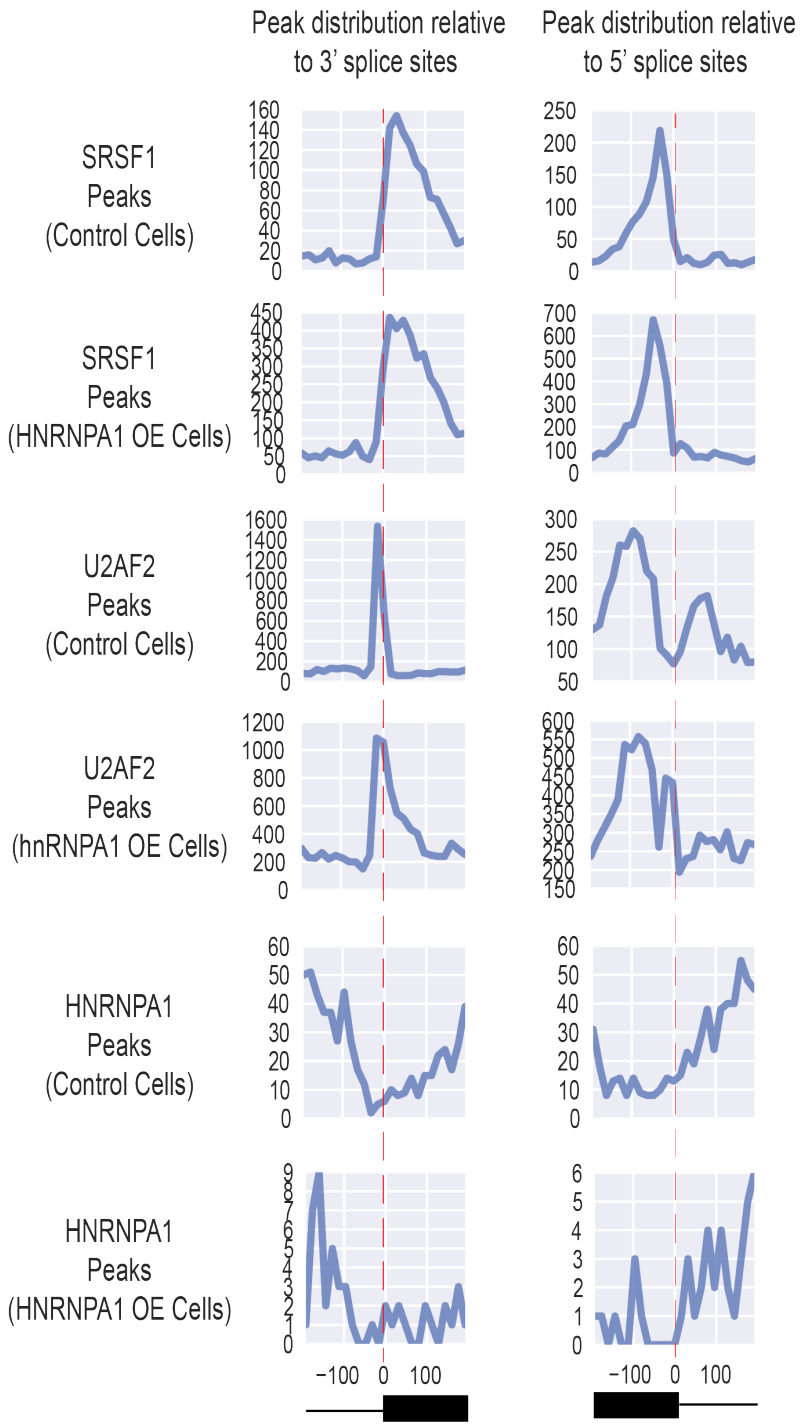

Supplemental Fig. 3. Distribution of HNRNPA1, SRSF1 and U2AF2 peaks relative to splice sites. The frequency of peaks occurring at different positions relative to splice sites is shown for each protein under control and HNRNPA1 over-expression conditions.

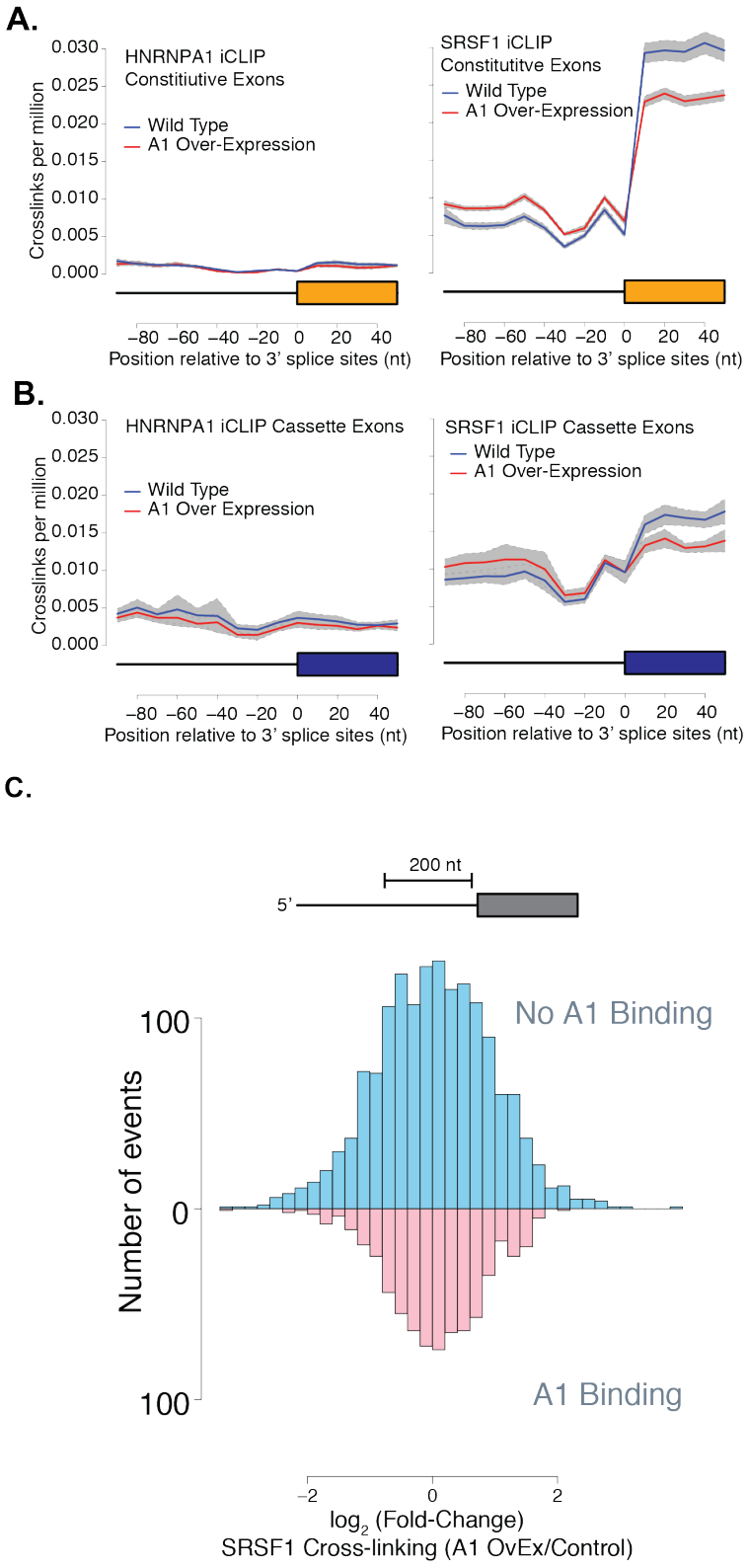

Supplemental Fig. 4. Distribution of SRSF1 and HNRNPA1 crosslinking sites relative to 3' splice sites in control and HNRNPA1 over-expressing HEK293T cells. (A, B) Normalized crosslinking distribution for HNRNPA1 and SRSF1 (right and left panels, respectively) in wild-type (blue line) and HNRNPA1 overexpression cell lines (red line) with 95% confidence interval (gray area). Data is divided between constitutive **(A)** and skipped **(B)** exons. **(C)** Nature log fold change distribution of SRSF1 within 200bp intron regions near 3' splice sites of cassette exons. Blue bars correspond to annotated alternative splicing events with no evidence of HNRNPA1 crosslinking in either condition and pink represents annotated events with detectable HNRNPA1 crosslinking.

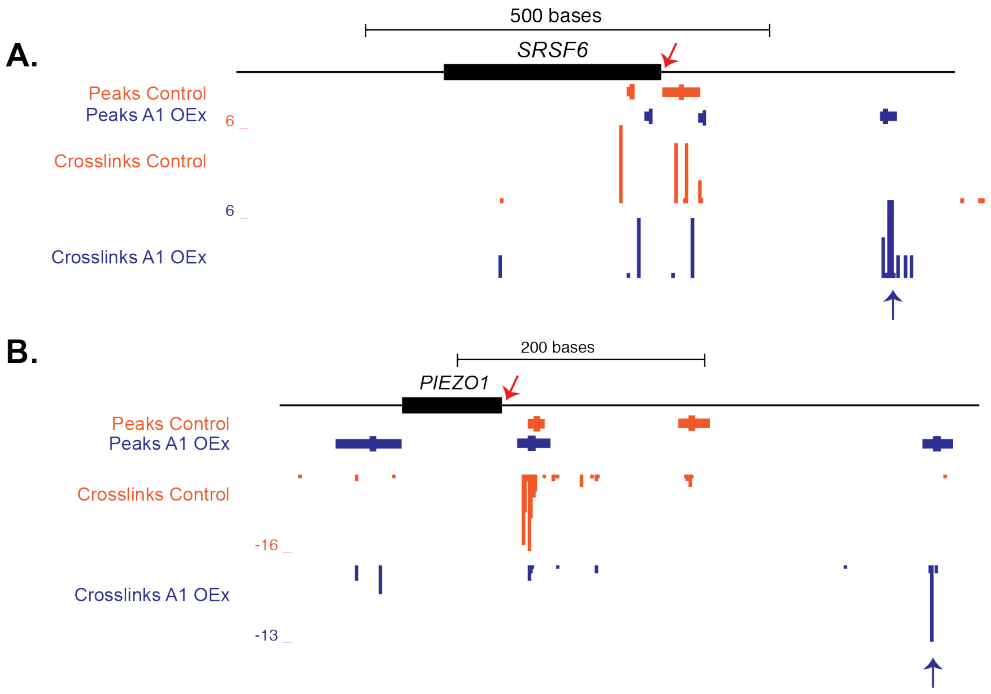

Supplemental Fig. 5. Examples of HNRNPA1-dependent modulation of U2AF2 crosslinking. UCSC genome browser examples of two genes *SRSF6* **(A)** and *PIEZO1* **(B)** and iCLIP read coverage data for U2AF2 under control and HNRNPA1 overexpression. Alternative splicing changes can be observed in figure 3 (*SRSF6*) and supplemental figures 13 and 16 (*PEIZO1* and *SRSF6*, respectively).

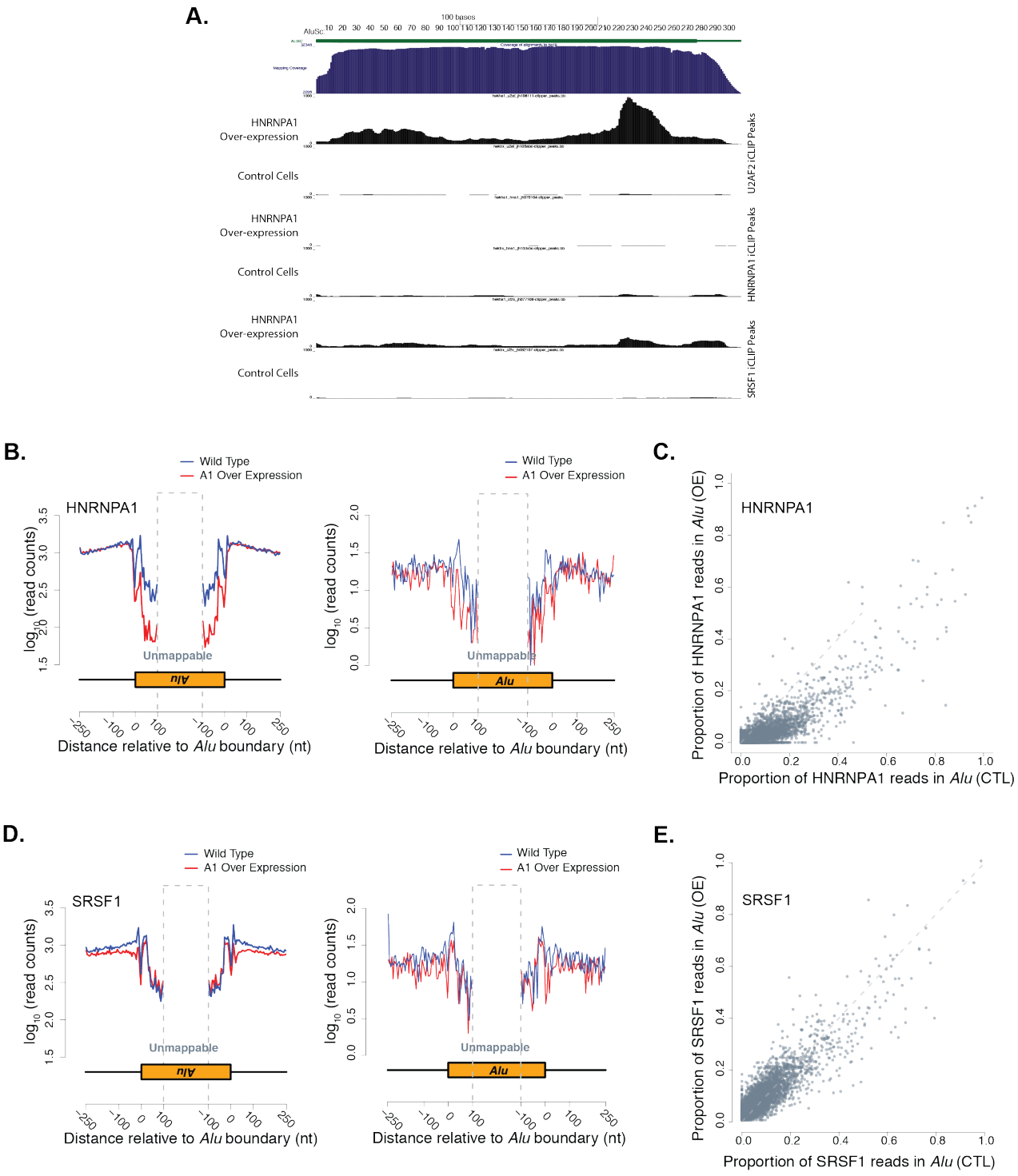

Supplemental Fig. 6. HNRNPA1 over-expression correlates with global redistribution of U2AF2 signal to *Alu* RNA elements. (A) Distribution of aggregated U2AF2, HNRNPA1, and SRSF1 iCLIP peaks on *Alu* subtype *AluSc* under control and HNRNPA1 over-expression conditions. **(B, D)** Aggregated crosslinking sites on *Alu* elements and nearby regions for **(B)** HNRNPA1 and **(D)** SRSF1. Blue represents wild-type binding of the given RNA binding protein and red represents HNRNPA1 over-expression of the $\log_{10}$ number of iCLIP read counts across all anti-sense (left graph) and sense (right graph) *Alu* elements.**(C, E)** Scatter plot of all human cassette exons measuring the proportion of **(C)** HNRNPA1 and **(E)** SRSF1 iCLIP crosslinks found within *Alu* elements relative to the total number of crosslinks observed throughout the alterative event.

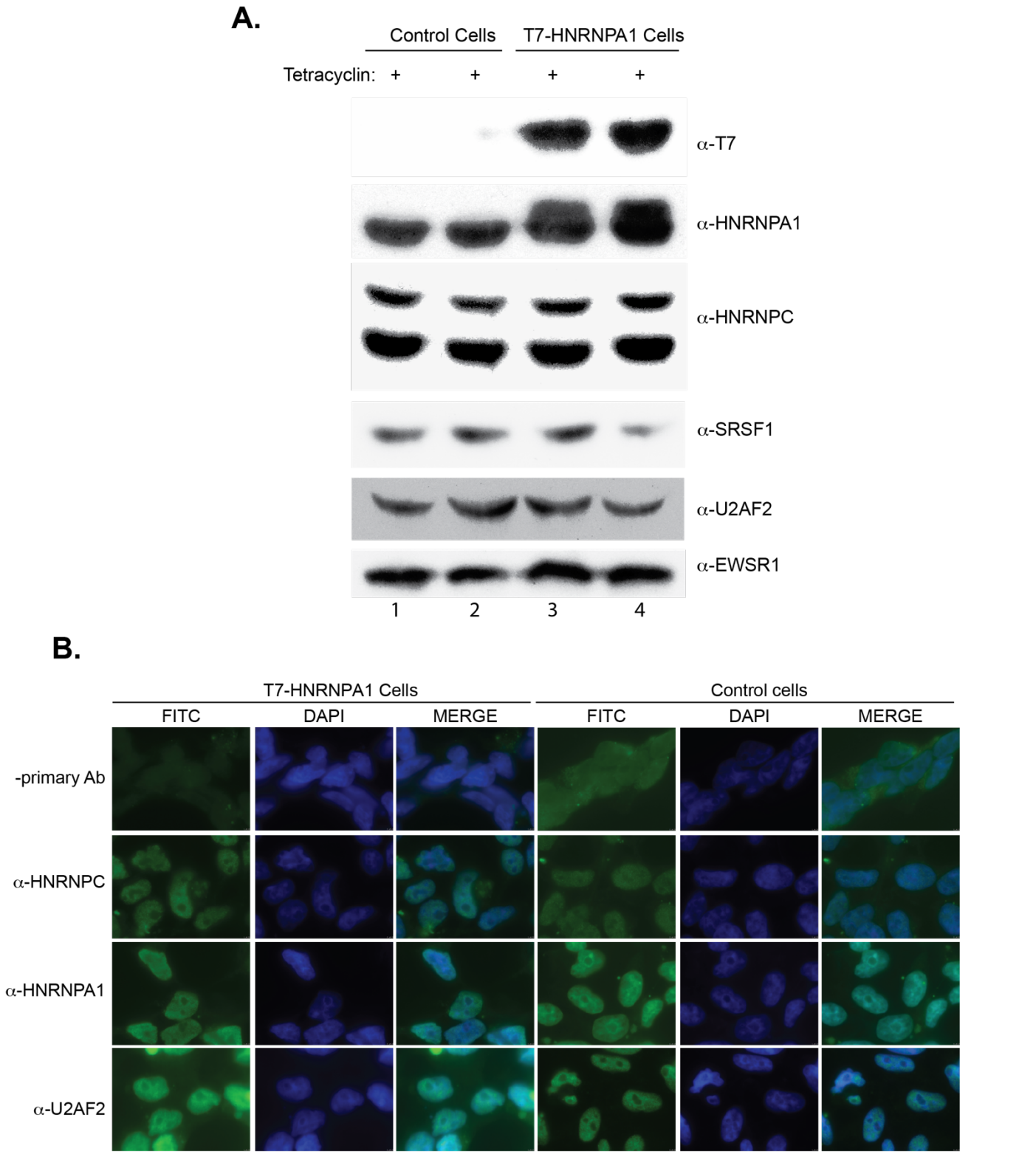

Supplemental Fig. 7. HNRNPC protein levels and sub-cellular localization are not affected by HNRNPA1 over-expression. (A) Nuclear extracts were subjected to SDS-PAGE and transferred to nitrocellulose blotting paper. Samples were interrogated with anitbodies for α-T7 peptide tag (with which overexpressed HNRNPA1 has been tagged), α-HNRNPA1 (4B10; Santa Cruz Biotechnology), α-SRSF1 (96;Santa Cruz Biotechnology), α-U2AF2 (MC3;Santa Cruz Biotechnology), α-HNRNPC1/C2 (Santa Cruz Biotechnology, 4F4) and α-EWSR1 (C-9; Santa Cruz Biotechnology) as positive control. **(B)** Immuno-staining of control HEK293T cells or HNRNPA1 over-expression cells with α-HNRNPC1/C2, α-HNRNPA1 and anti-U2AF2.

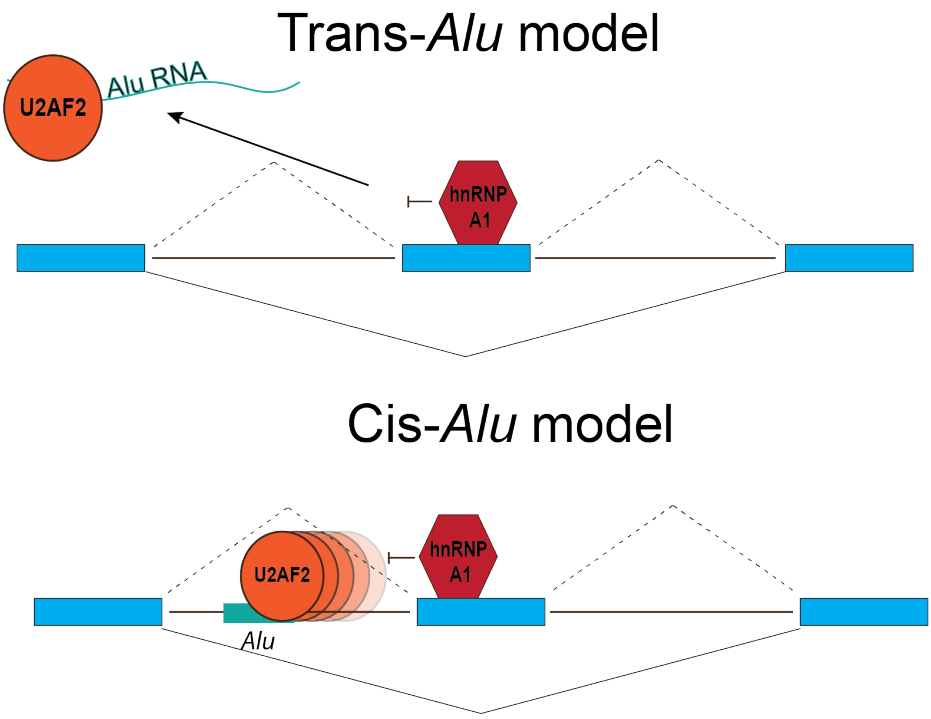

Supplemental Fig. 8. Trans- vs. Cis-*Alu* competition model of U2AF2 redistribution. Model representing two potential modes by which U2AF2 may associate with *Alu* RNA: trans- competition suggests U2AF2 binds to *Alu* elements on other RNAs, while a cis-competition suggest U2AF2 binds to *Alu* elements within the same RNAs that a particular exon is associated

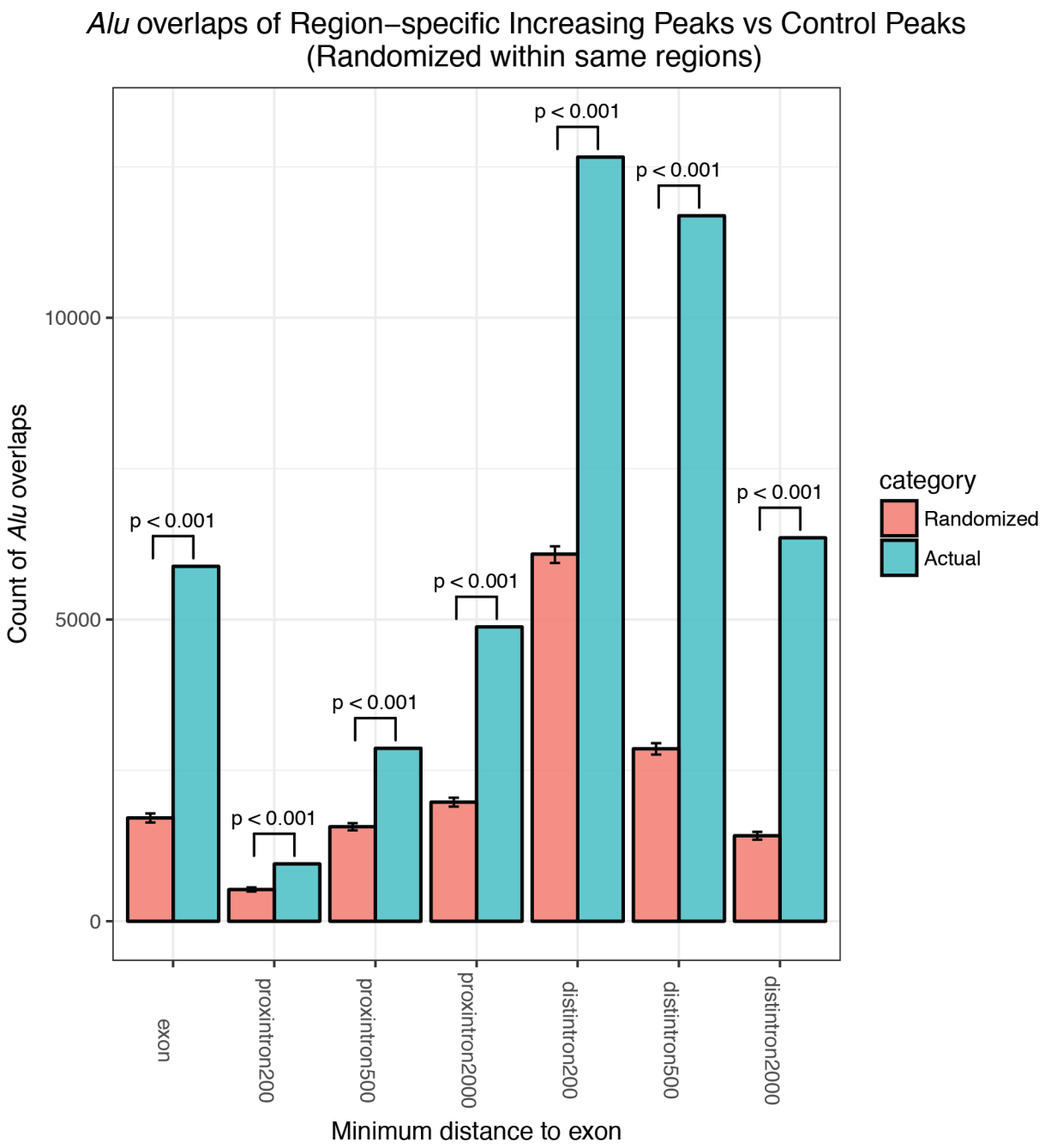

Supplemental Fig. 9. U2AF2 Peaks in proximal and distal introns are enriched in positions overlapping *Alu* elements. Comparison of observed (Actual) *Alu*-element overlap of increasing distal intronic peaks to the *Alu*-element overlap by peaks randomly shuffled (Randomized) within the same population of distal intronic regions. Random shuffling was performed 1000 times to create a null distribution for each definition of distal intronic regions (> 200, 500, or 2000 bp from the nearest exon boundary).

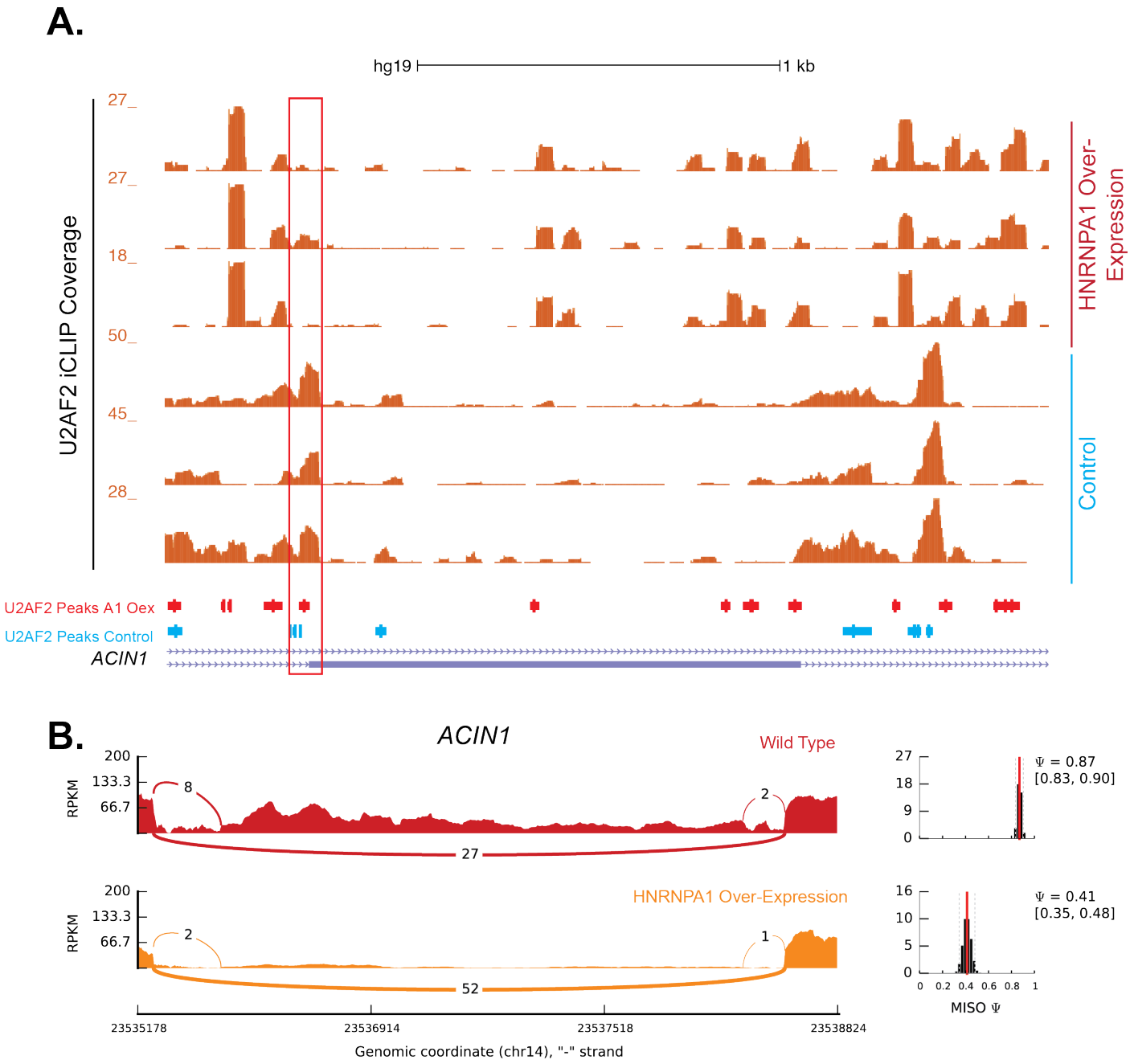

Supplemental Fig. 10. HNRNPA1-dependent modulation of U2AF2 crosslinking and alternative splicing of *ACIN1*. (A) Genome browser snap shot of iCLIP read coverage surrounding alternative exon. The 3' splice site is indicated by a red box. **(B)** Sashimi plot showing read coverage, junction read counts and estimated percent spliced in values (PSI) from aggregated RNA seq data obtained from control (red) or HNRNPA1 over-expression HEK293T cells (gold).

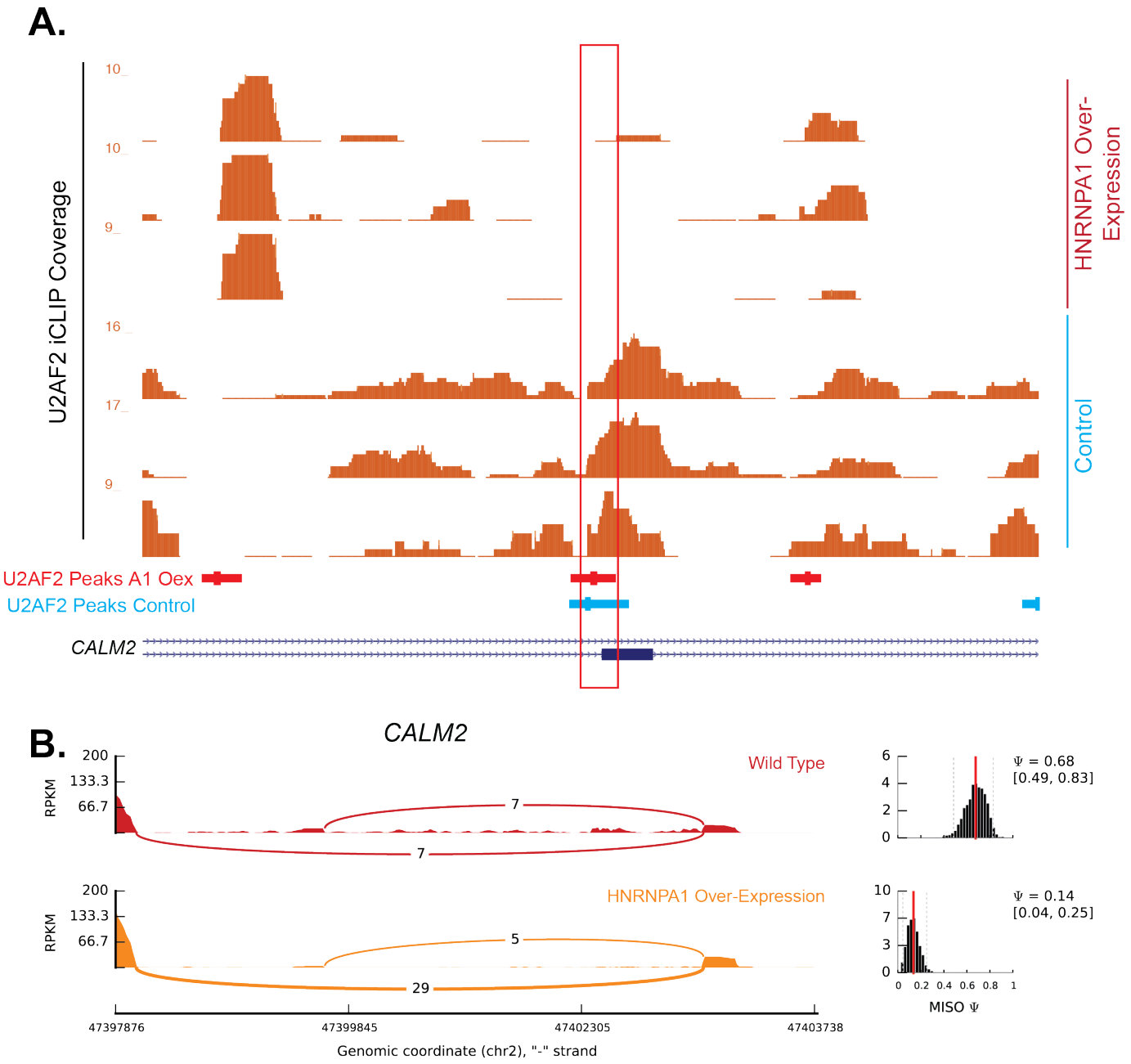

Supplemental Fig. 11. HNRNPA1-dependent modulation of U2AF2 crosslinking and alternative splicing of *CALM2*. (A) Genome browser snap shot of iCLIP read coverage surrounding alternative exon. The 3' splice site is indicated by a red box. **(B)** Sashimi plot showing read coverage, junction read counts and estimated percent spliced in values (PSI) from aggregated RNA seq data obtained from control (red) or HNRNPA1 over-expression HEK293T cells (gold).

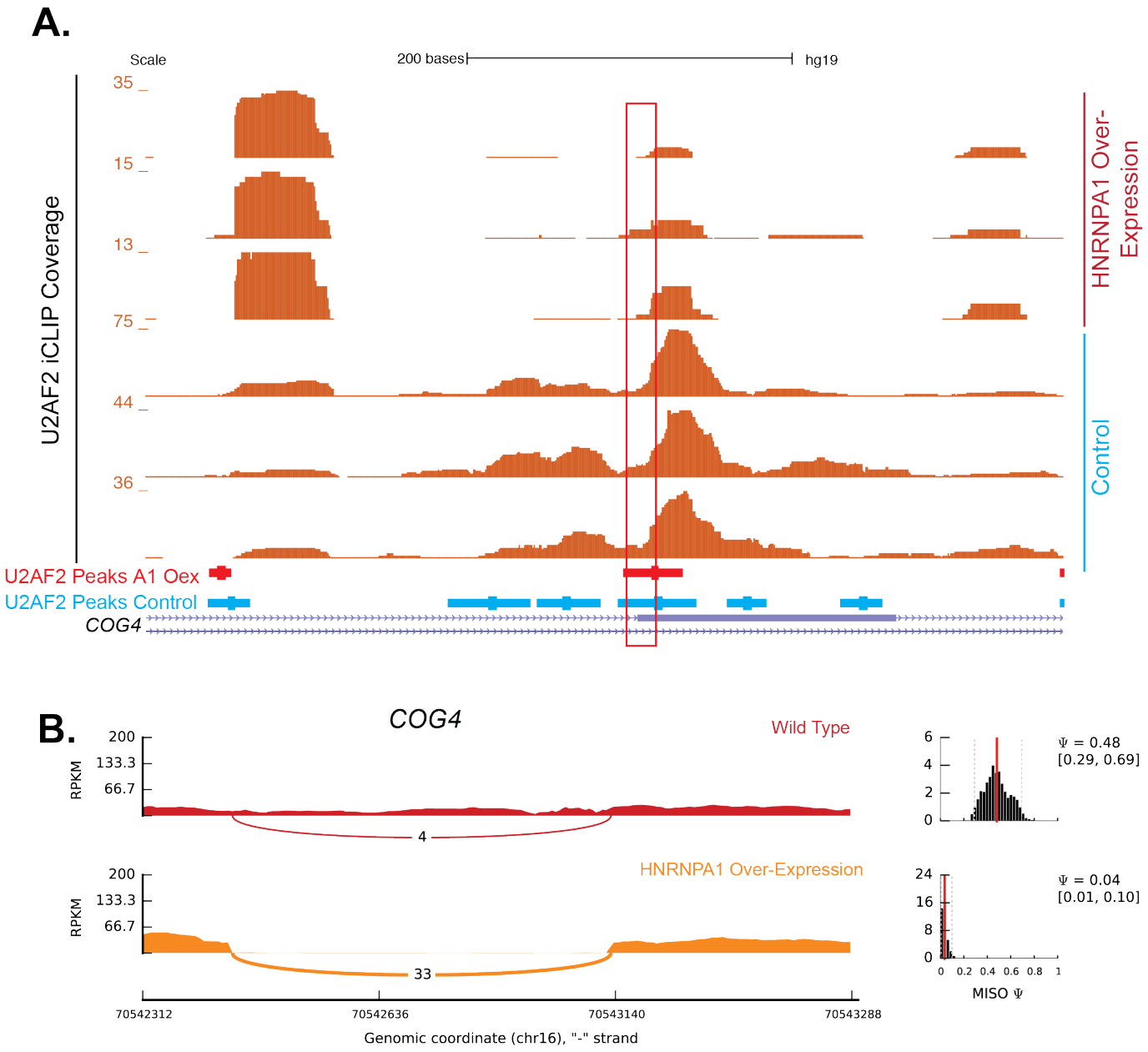

Supplemental Fig. 12. HNRNPA1-dependent modulation of U2AF2 crosslinking and alternative splicing of *COG4*. (A) Genome browser snap shot of iCLIP read coverage surrounding alternative exon. The 3' splice site is indicated by a red box. **(B)** Sashimi plot showing read coverage, junction read counts and estimated percent spliced in values (PSI) from aggregated RNA seq data obtained from control (red) or HNRNPA1 over-expression HEK293T cells (gold).

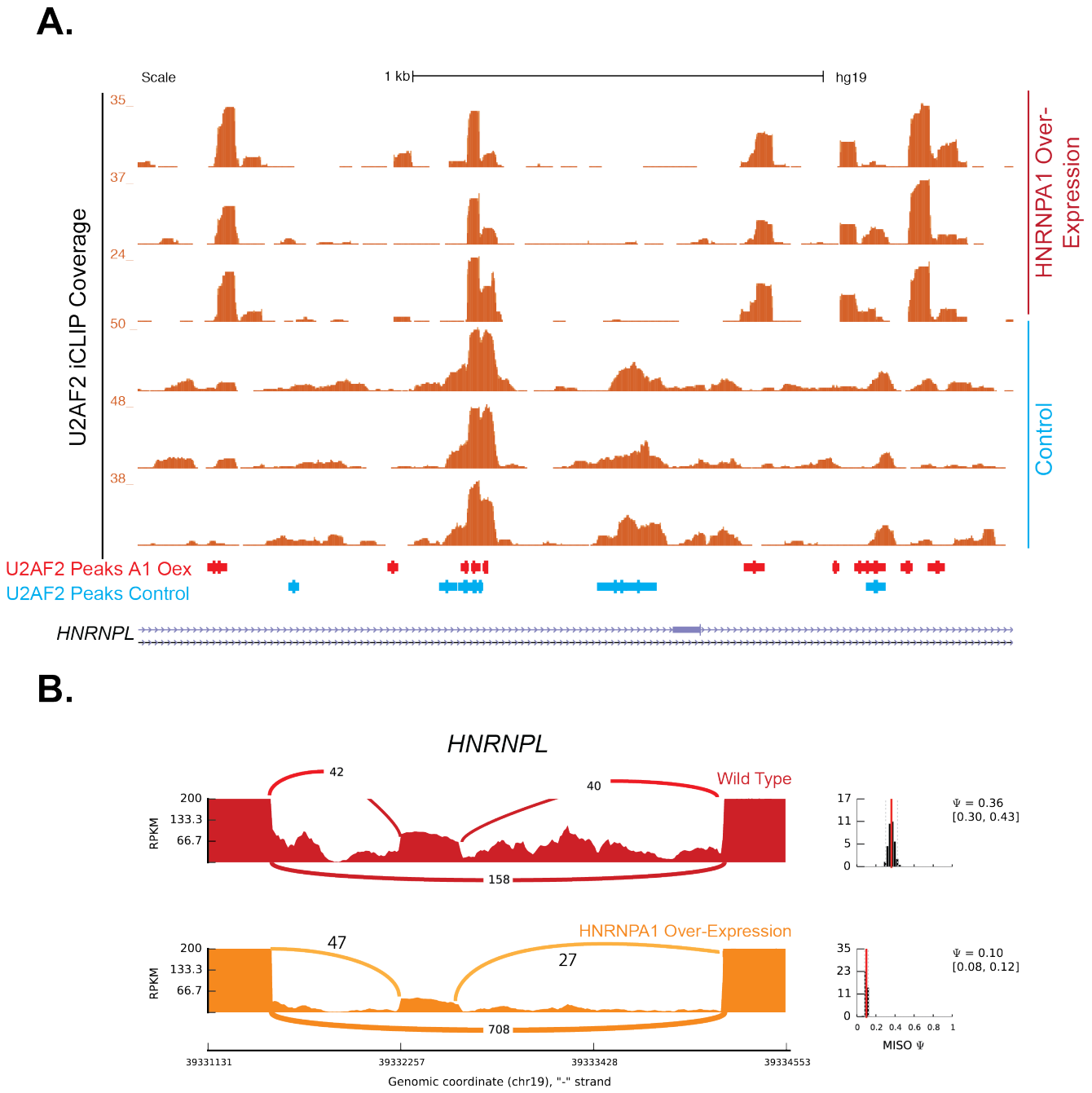

Supplemental Fig. 13. HNRNPA1-dependent modulation of U2AF2 crosslinking and alternative splicing of *HNRNPL*. (A) Genome browser snap shot of iCLIP read coverage surrounding alternative exon. The 3' splice site is indicated by a red box. **(B)** Sashimi plot showing read coverage, junction read counts and estimated percent spliced in values (PSI) from aggregated RNA seq data obtained from control (red) or HNRNPA1 over-expression HEK293T cells (gold).

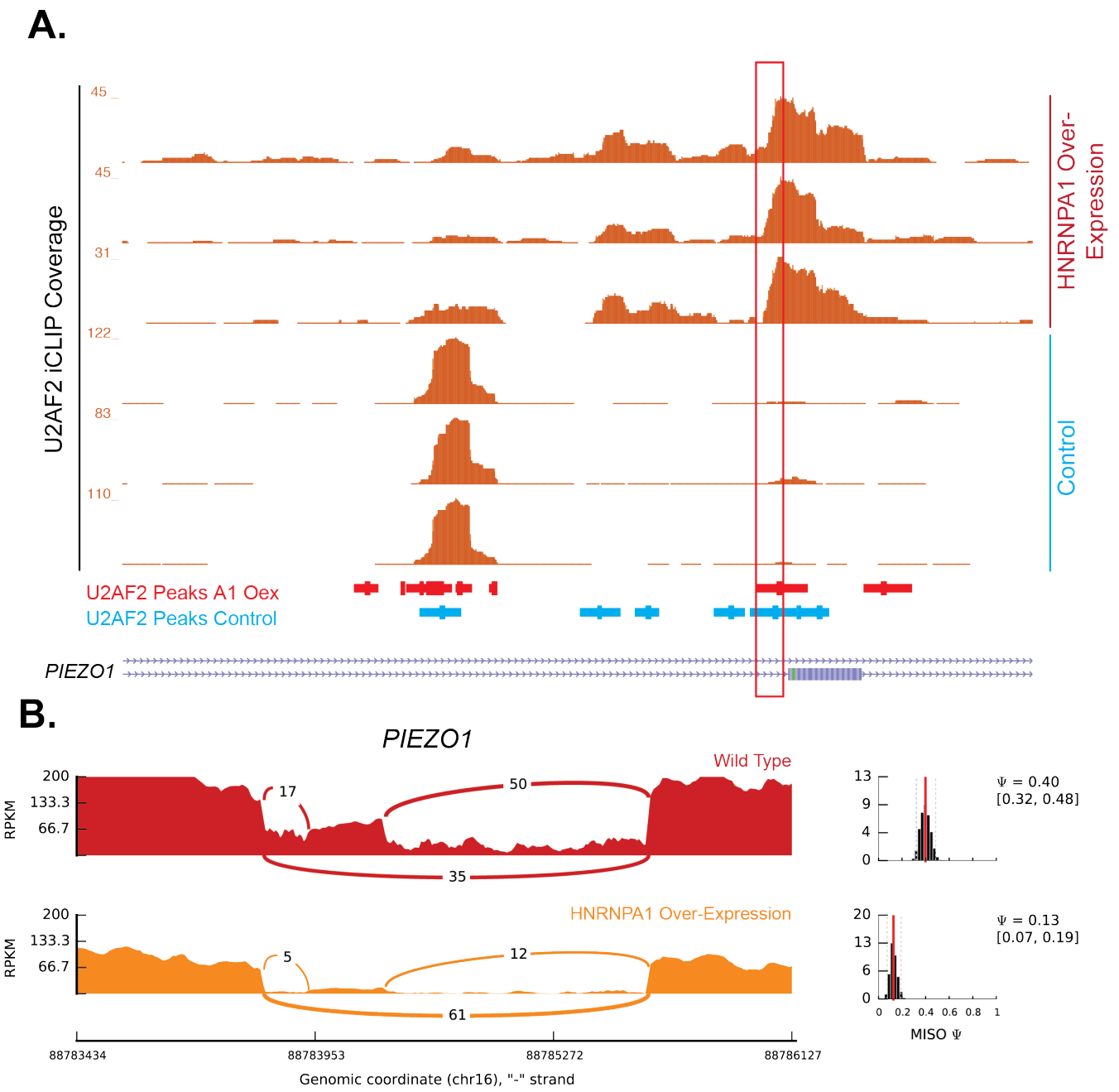

Supplemental Fig. 14. HNRNPA1-dependent modulation of U2AF2 crosslinking and alternative splicing of *PIEZO1*. (A) Genome browser snap shot of iCLIP read coverage surrounding alternative exon. The 3' splice site is indicated by a red box. **(B)** Sashimi plot showing read coverage, junction read counts and estimated percent spliced in values (PSI) from aggregated RNA seq data obtained from control (red) or HNRNPA1 over-expression HEK293T cells (gold).

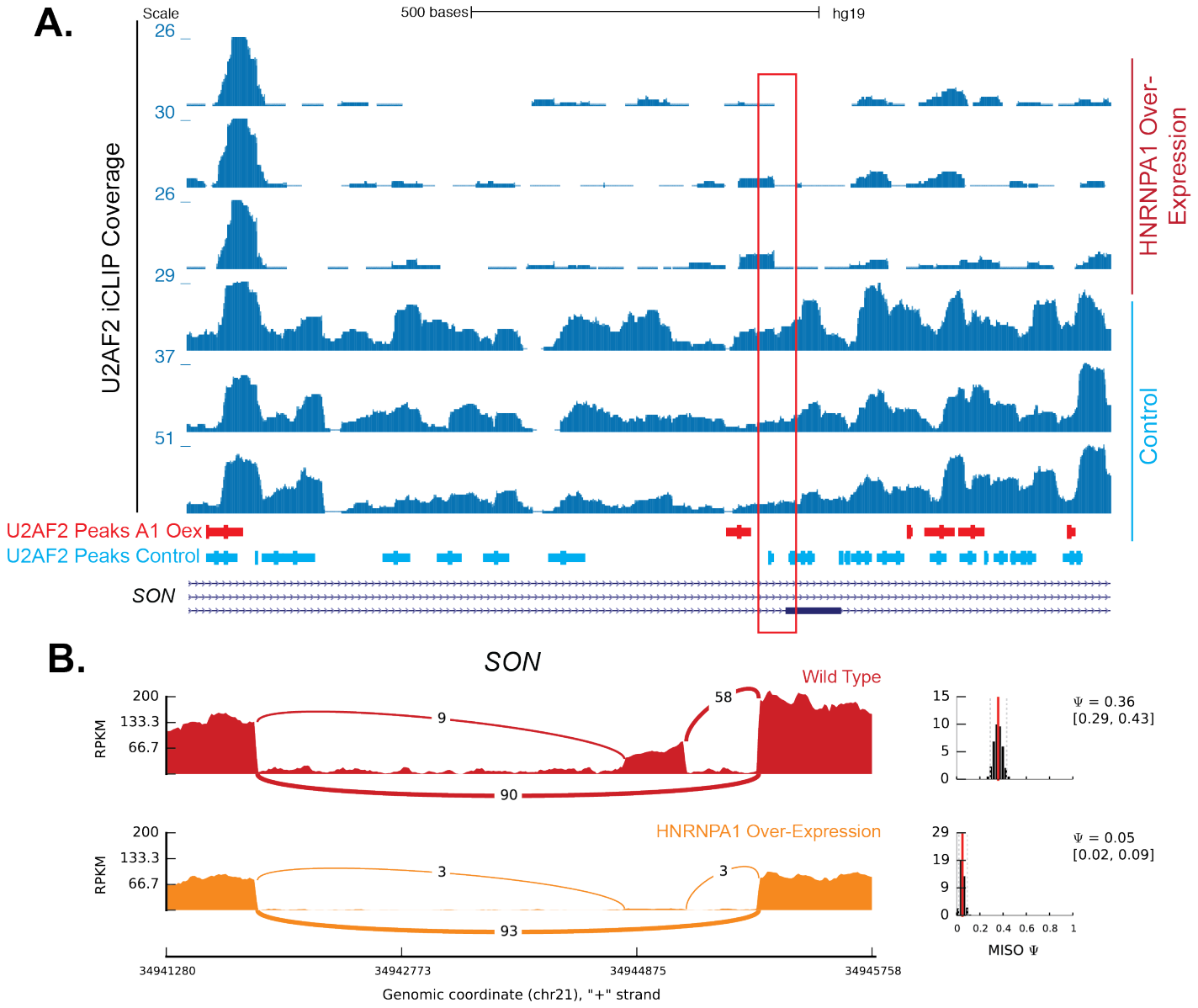

Supplemental Fig. 15. HNRNPA1-dependent modulation of U2AF2 crosslinking and alternative splicing of *SON*. (A) Genome browser snap shot of iCLIP read coverage surrounding alternative exon. The 3' splice site is indicated by a red box. **(B)** Sashimi plot showing read coverage, junction read counts and estimated percent spliced in values (PSI) from aggregated RNA seq data obtained from control (red) or HNRNPA1 over-expression HEK293T cells (gold).

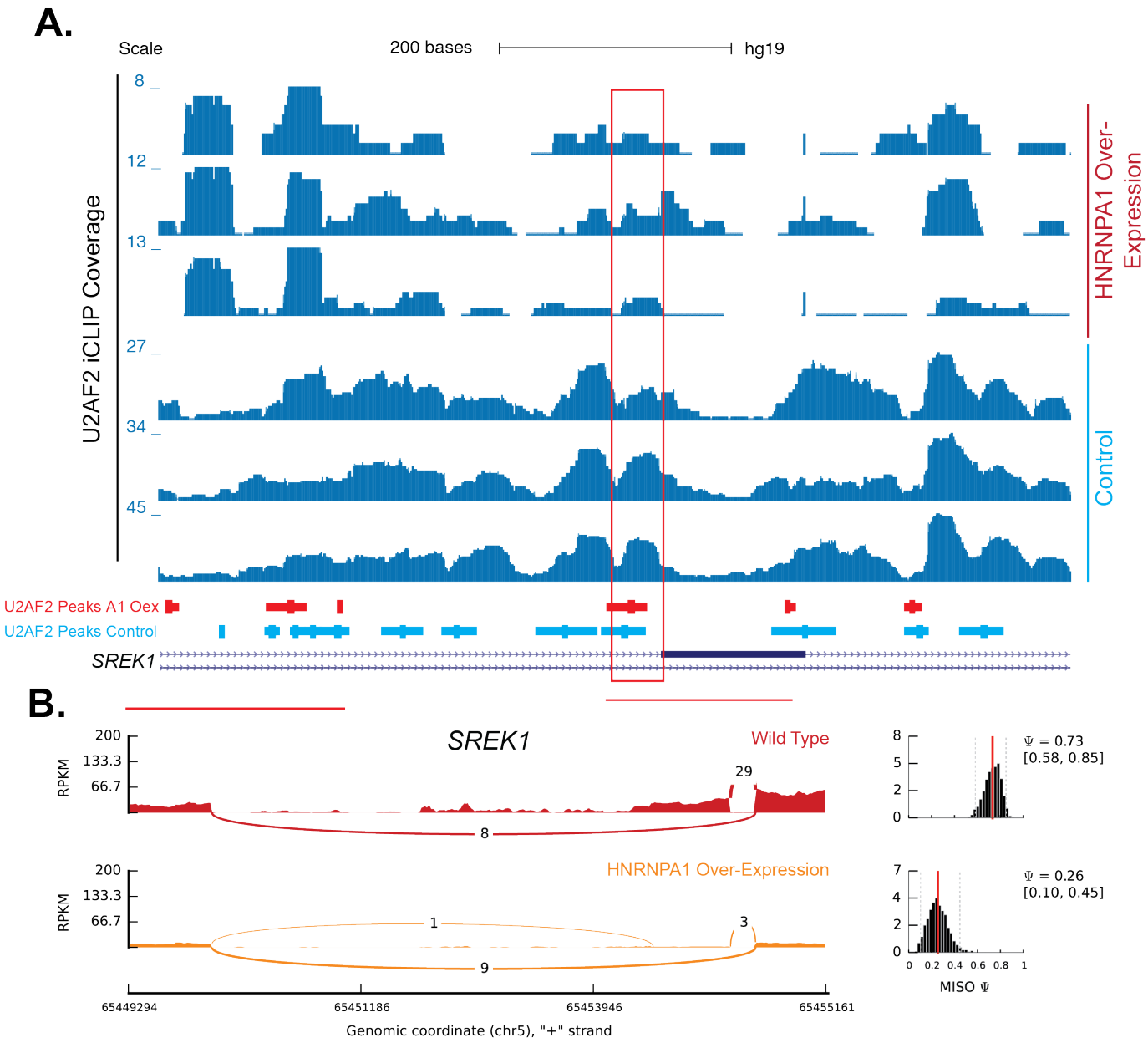

Supplemental Fig. 16. HNRNPA1-dependent modulation of U2AF2 crosslinking and alternative splicing of *SREK1*. (A) Genome browser snap shot of iCLIP read coverage surrounding alternative exon. The 3' splice site is indicated by a red box. **(B)** Sashimi plot showing read coverage, junction read counts and estimated percent spliced in values (PSI) from aggregated RNA seq data obtained from control (red) or HNRNPA1 over-expression HEK293T cells (gold).

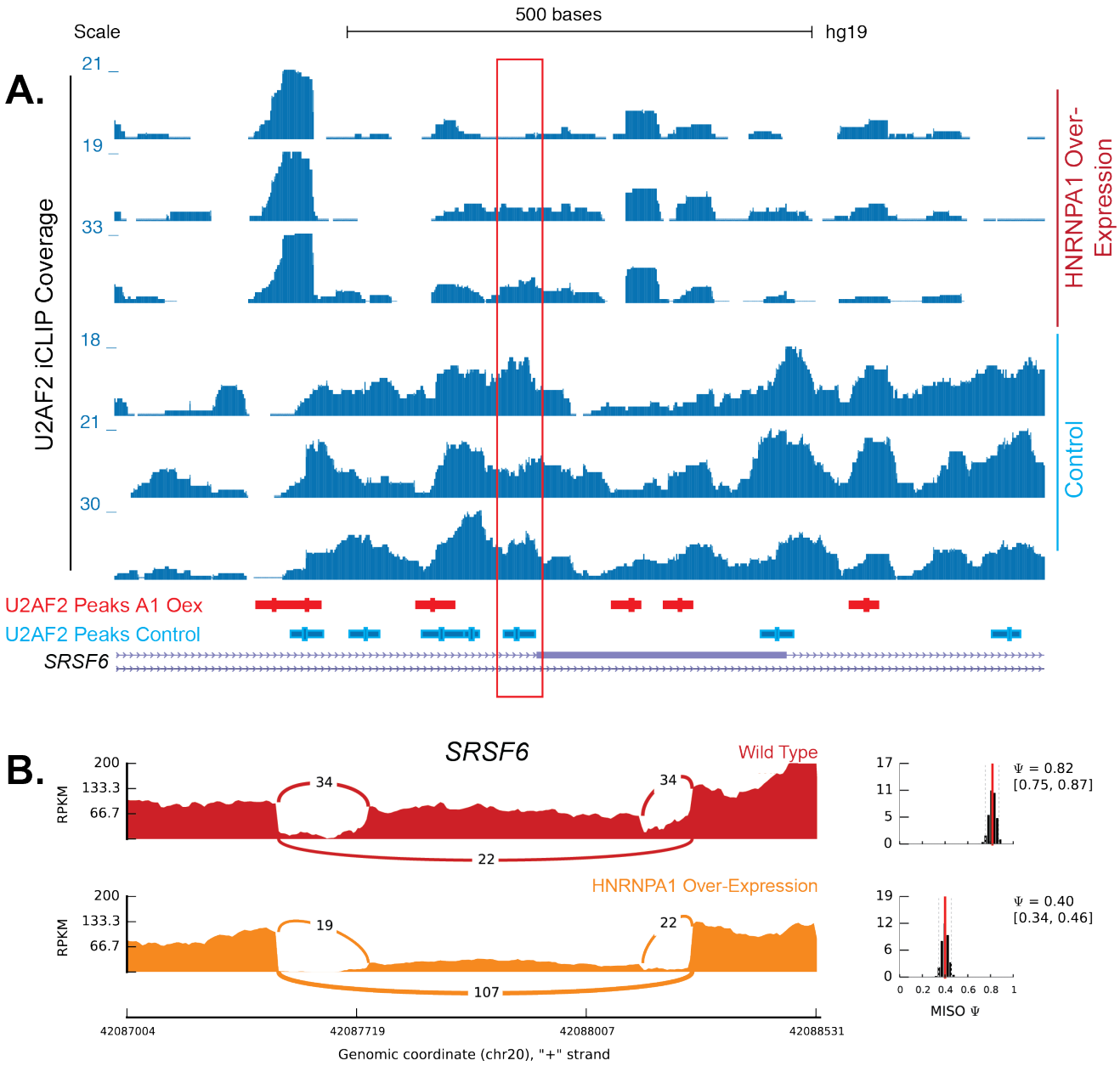

Supplemental Fig. 17. HNRNPA1-dependent modulation of U2AF2 crosslinking and alternative splicing of *SRSF6*. (A) Genome browser snap shot of iCLIP read coverage surrounding alternative exon. The 3' splice site is indicated by a red box. **(B)** Sashimi plot showing read coverage, junction read counts and estimated percent spliced in values (PSI) from aggregated RNA seq data obtained from control (red) or HNRNPA1 over-expression HEK293T cells (gold).

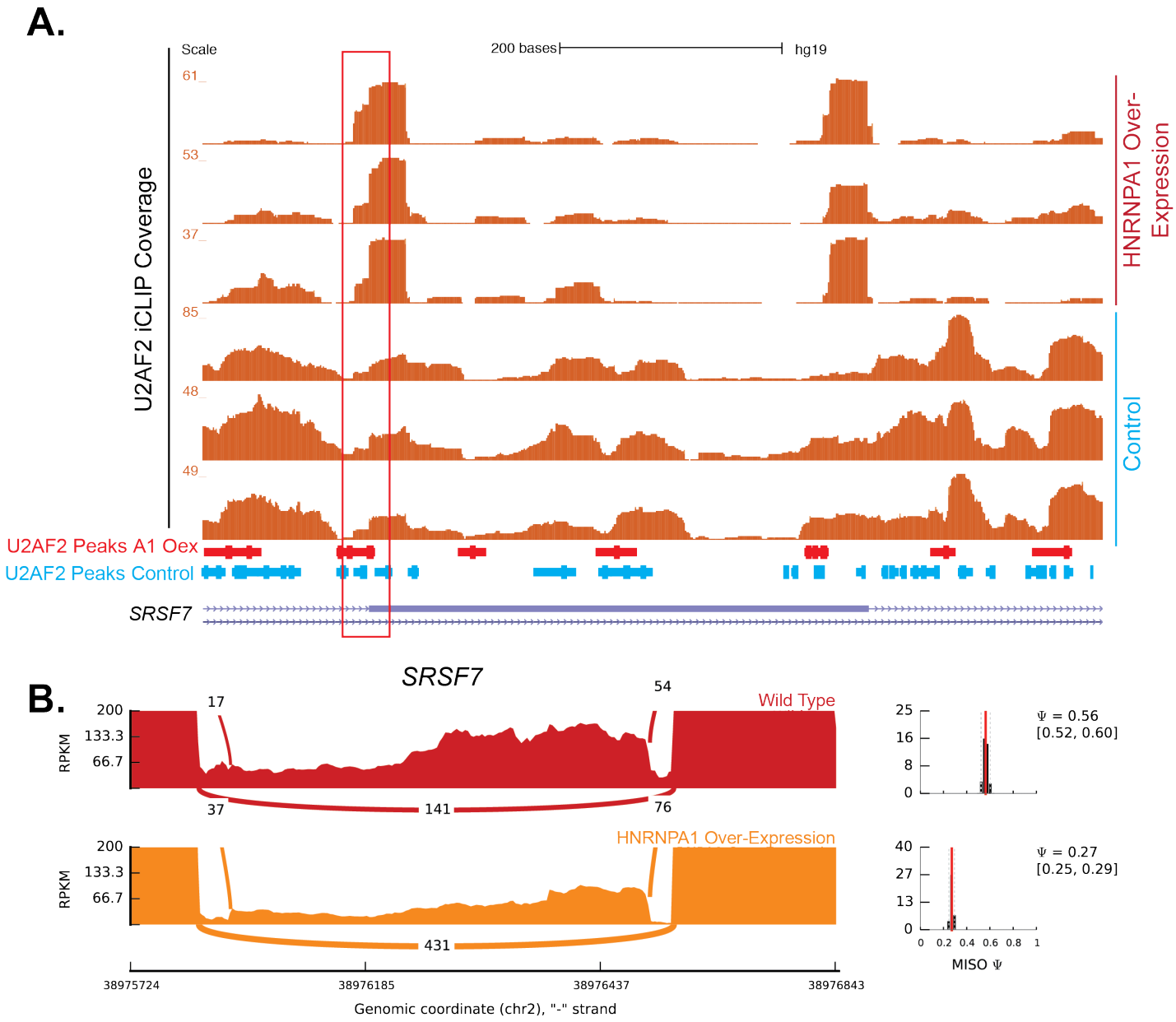

Supplemental Fig. 18. HNRNPA1-dependent modulation of U2AF2 crosslinking and alternative splicing of *SRSF7*. (A) Genome browser snap shot of iCLIP read coverage surrounding alternative exon. The 3' splice site is indicated by a red box. **(B)** Sashimi plot showing read coverage, junction read counts and estimated percent spliced in values (PSI) from aggregated RNA seq data obtained from control (red) or HNRNPA1 over-expression HEK293T cells (gold).

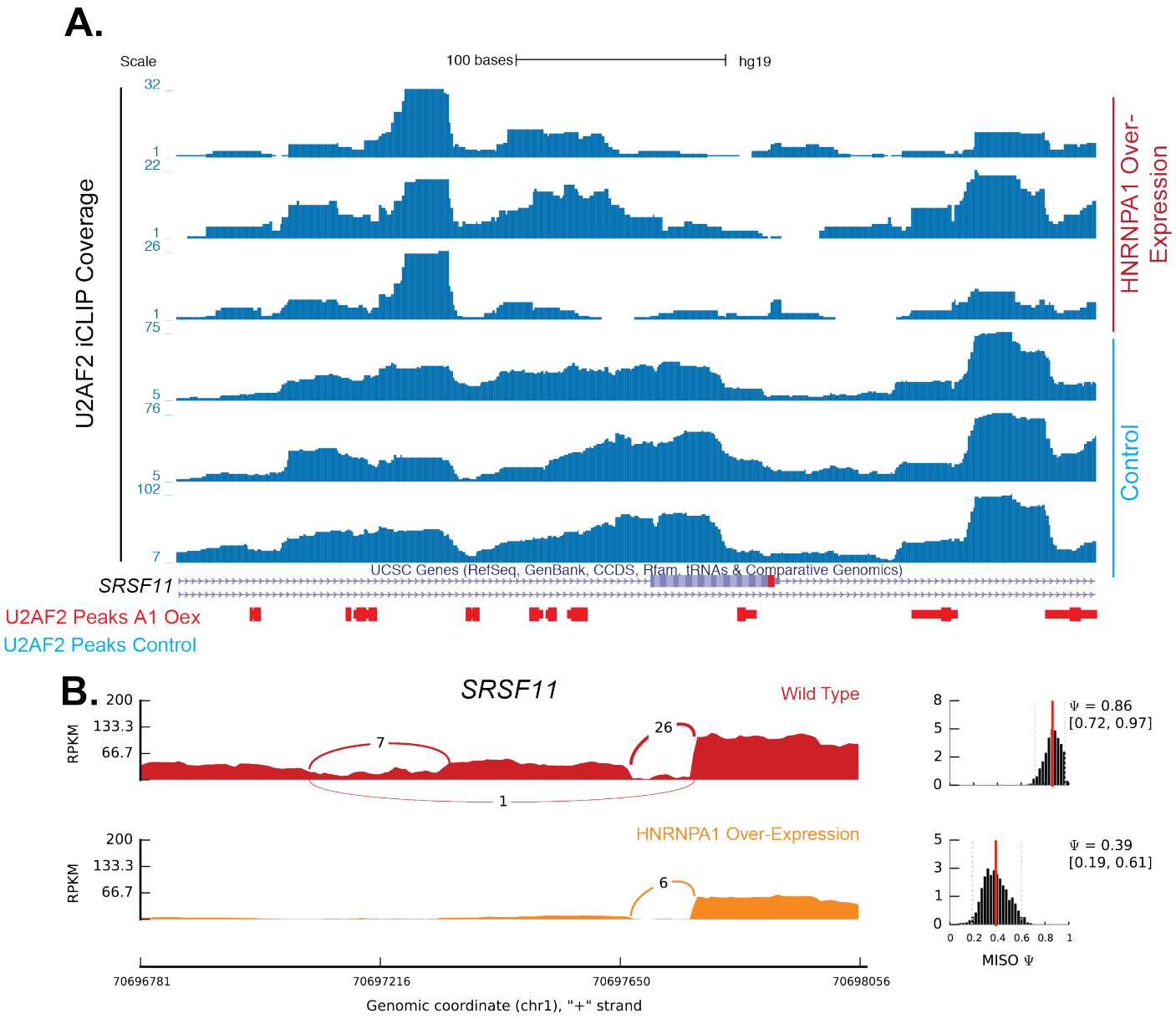

Supplemental Fig. 19. HNRNPA1-dependent modulation of U2AF2 crosslinking and alternative splicing of *SRSF11*. (A) Genome browser snap shot of iCLIP read coverage surrounding alternative exon. The 3' splice site is indicated by a red box. **(B)** Sashimi plot showing read coverage, junction read counts and estimated percent spliced in values (PSI) from aggregated RNA seq data obtained from control (red) or HNRNPA1 over-expression HEK293T cells (gold).

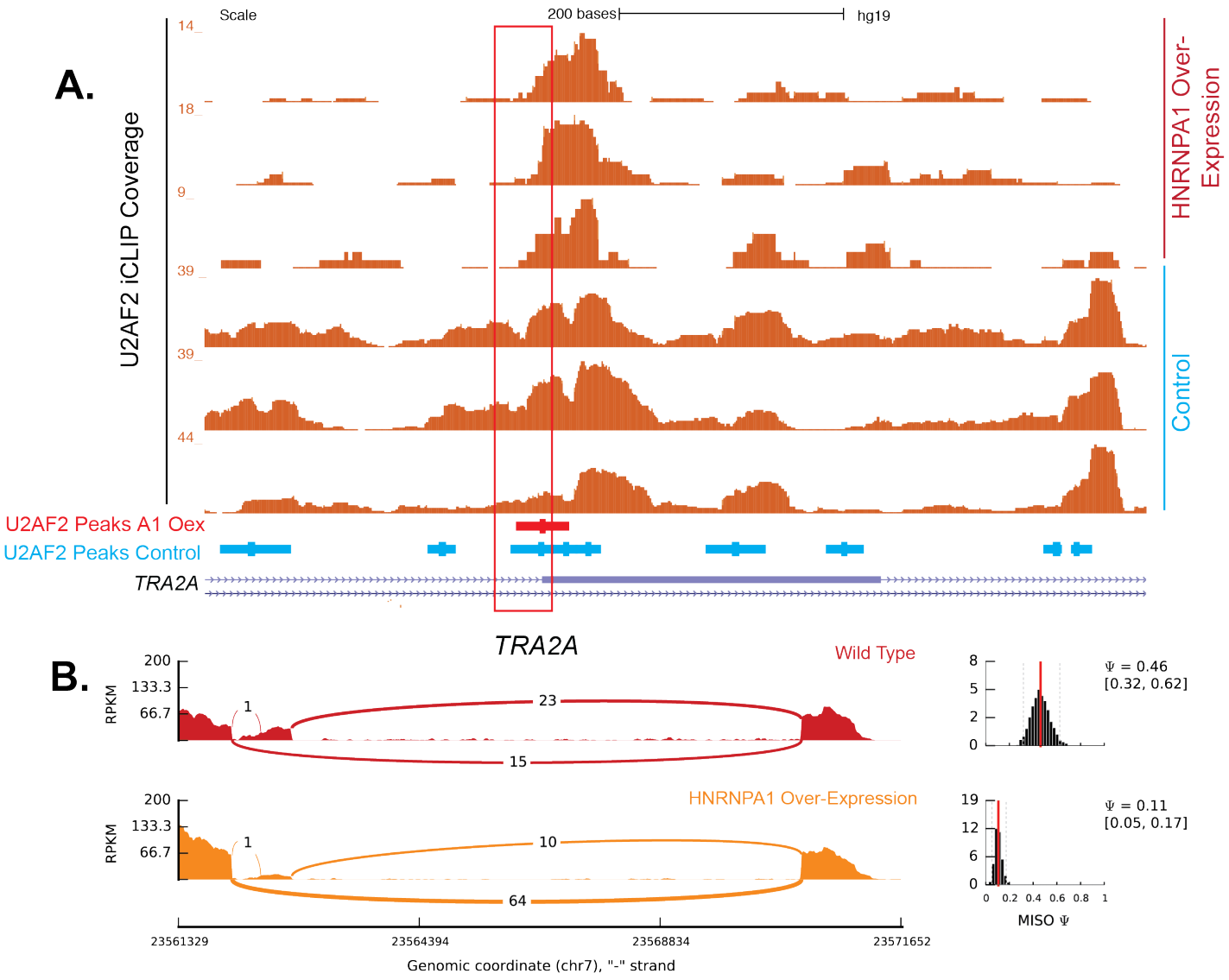

Supplemental Fig. 20. HNRNPA1-dependent modulation of U2AF2 crosslinking and alternative splicing of *TRA2A*. (A) Genome browser snap shot of iCLIP read coverage surrounding alternative exon. The 3' splice site is indicated by a red box. **(B)** Sashimi plot showing read coverage, junction read counts and estimated percent spliced in values (PSI) from aggregated RNA seq data obtained from control (red) or HNRNPA1 over-expression HEK293T cells (gold).